Three-Dimensional Analysis of Human Laryngeal and Tracheobronchial Cartilages during the Late Embryonic and Early Fetal Period

AUTHOR(S):

Yamasaki, Yu; Kanahashi, Toru; Yamada, Shigehito; Männer, Jörg; Takakuwa, Tetsuya

CITATION:

Yamasaki, Yu ...[et al]. Three-Dimensional Analysis of Human Laryngeal and Tracheobronchial Cartilages during the Late Embryonic and Early Fetal Period. Cells Tissues Organs 2022, 211(1): 1-15

ISSUE DATE:

2022-01

URL:

http://hdl.handle.net/2433/277284

Cells Tissues Organs

Developmental Biology / Research Article

Cells Tissues Organs 2022;211:1–15
DOI: 10.1159/000519160

Received: May 11, 2021
Accepted: July 17, 2021
Published online: August 26, 2021

Three-Dimensional Analysis of Human Laryngeal and Tracheobronchial Cartilages during the Late Embryonic and Early Fetal Period

Yu Yamazaki[a] Toru Kanahashi[a] Shigehito Yamada[a, b] Jörg Männer[c] Tetsuya Takakuwa[a]

[a]Human Health Science, Kyoto University Graduate School of Medicine, Kyoto, Japan; [b]Congenital Anomaly Research Center, Kyoto University Graduate School of Medicine, Kyoto, Japan; [c]Institute of Anatomy and Embryology, UMG, Georg-August-University of Göttingen, Göttingen, Germany

Keywords
3D analysis · Human embryonic and early fetal period · Laryngeal cartilages · Tracheobronchial cartilages

Abstract
Laryngeal and tracheobronchial cartilages are present as unique U-shaped forms around the respiratory tract and contribute to the formation of rigid structures required for the airway. Certain discrepancies still exist concerning cartilage formation in humans. To visualize the accurate timeline of cartilage formation, tracheobronchial and laryngeal cartilages were 3D reconstructed based on serial tissue sections during the embryonic period (Carnegie stage [CS] 18–23) and early fetal period (crown rump length [CRL] = 35–45 mm). The developmental phases of the cartilage were estimated by histological studies, which were performed on the reconstructed tissue sections. The hyoid greater horns were recognizable at CS18 (phase 2). Fusion of 2 chondrification centers in the mid-sagittal region was observed at CS19 in the hyoid bone, at CS20 in the cricoid cartilage, and in the specimen with CRL 39 mm in the thyroid cartilage. Phase 3 differentiation was observed at the median part of the hyoid body at CS19, which was the earliest among all other laryngeal and tracheobronchial cartilages. Most of the laryngeal cartilages were in phase 3 differentiation at CS22 and in phase 4 differentiation at CS23. The U-shaped tracheobronchial cartilages with phase 2 differentiation covered the entire extrapulmonary region at CS20. Phase 3 differentiation started on the median section and propagates laterally at CS21. The tracheobronchial cartilages may form simultaneously during the embryonic period at CS22-23 and early fetal periods, similar to adults in number and distribution. The spatial propagation of the tracheal cartilage differentiation provided in the present study indicates that cartilage differentiation may have propagated differently on phase 2 and phase 3. This study demonstrates a comprehensible timeline of cartilage formation. Such detailed information of the timeline of cartilage formation would be useful to improve our understanding of the development and pathophysiology of congenital airway anomalies.

Introduction

Cartilage is a highly specialized, dense type of connective tissue consisting of cells (chondrocytes) that produce a firm, abundant matrix (particularly type 2 collagen) in

karger@karger.com
www.karger.com/cto

Correspondence to:
Tetsuya Takakuwa, tez@hs.med.kyoto-u.ac.jp

which they are embedded [O'Rahilly and Müller, 2001a]. Most cartilage plays a role in providing a template for the developing skeleton, which is essential for the growth of bones both prenatally and postnatally. Cartilage in adults is found mainly at the end of the bone, forming joints to the adjacent bones. Meanwhile, several cartilages are found as unique U-shaped forms around the respiratory tract, including laryngeal regions (thyroid cartilage) and tracheobronchial cartilages, which contribute to the rigid structure that maintains airway patency. A comparative anatomical study indicated that these U-shaped cartilages might be homologous to the brachial arches in fish [Brien and Dalcq, 1954], although the origin of each cartilage type in humans remained controversial [Zaw-Tun and Burdi, 1985; O'Rahilly and Müller, 2001b; Rodríguez-Vázquez et al., 2011].

Over a century ago, Bardeen [1910] and Lisser [1911] described the development of the human larynx region, including the hyoid bone and laryngeal cartilages. The development of the human larynx has been reanalyzed in recent several studies [Zaw-Tun and Burdi, 1985; Rodríguez-Vázquez et al., 2011; de Bakker et al., 2018]. As far as cartilage formation is concerned, some discrepancies remain regarding the timing of the initial appearance, site of cartilage center formation, and fusion in the mid-sagittal region.

Methods of reconstructing the inside of the bronchi, such as casts and injection preparations, have contributed to the advancement of studies concerning pulmonary structural anatomy. However, these methods ignore the structure of the pulmonary wall, resulting in limited information on the pulmonary wall, including pulmonary cartilages [Vanpeperstraete, 1973]. The study of the bronchial wall is still confined to histological studies [Bucher and Reid, 1961; Miller, 1966].

Congenital anomalies of the laryngeal and tracheal cartilages cause considerable morbidity and mortality in the pediatric population [Hartnick and Cotton, 2000]. An understanding of normal larynx and trachea cartilage development is still limited by the sparse knowledge available. In this study, the 3D construction of tracheobronchial cartilages and laryngeal cartilages was based on serial tissue sections. The developmental phases of the cartilage were estimated by histological studies and were mapped on the reconstructions. The goal of our study was to demonstrate a comprehensible timeline of detailed cartilage formation which would help to improve our understanding of the development and pathophysiology of congenital airway anomalies.

Materials and Methods

Human Embryo Specimens

At the Congenital Anomaly Research Center, Kyoto University Graduate School of Medicine, approximately 45,000 human specimens of embryos and fetuses, constituting the Kyoto Collection, are stored [Yamaguchi and Yamada, 2018]. Most specimens were obtained when pregnancy was terminated during the first trimester under the Maternity Protection Law of Japan. The specimens were collected from 1963 to 1995 according to the regulations pertaining to each period. For instance, written informed consent was not required from parents back then. Instead, parents provided verbal informed consent to have these specimens deposited, and each participant's consent was documented in the medical record. All specimens were anonymized and de-identified. Approximately 20% of the specimens were undamaged and well preserved. These embryos were measured, examined, and staged according to the criteria described by O'Rahilly and Müller [1987]. Whole embryonic specimens were fixed with 10% formalin, embedded in paraffin, and serially sectioned to a thickness of 10 μm. These specimens were stained with hematoxylin and eosin (HE), and the specimens were properly preserved. The Blechschmidt Collection, famous for its reconstructed models and a collection of over 20,000 fine microscopical slides, is located at the Center of Anatomy, University Medical Center Göttingen [Brand-Saberi et al., 2012]. Most slices are 10 μm thick and stained with HE [Miyazaki et al., 2018].

In this study, serial tissue sections of embryo specimens between CS18 and CS23 belonging to the Kyoto Collection ranged from 13.4 to 28.7 mm CRL (n = 15, 1–3 specimens per stage). For the early fetal period, 4 specimens of CRL 35, 39, 41, and 45 mm belonging to the Blechschmidt Collection were used. Only sagittal sections were selected as this would allow observations on both laryngeal and tracheal cartilages. For the tracheal cartilages; the segmentation, number of cartilages, and their branching formations were discernable, particularly at initial cartilage differentiation.

Digitization of the Histological Sections and 3D Reconstructions

Serial tissue sections (10-μm thick sagittal sections) of the embryos from the Kyoto Collection were digitized using an Olympus virtual slide system (VS120; Olympus Corporation, Tokyo, Japan). Serial tissue sections (10–25-μm thick sagittal sections) of fetuses from the Blechschmidt Collection were digitized using a flatbed scanner (CanoScan 9000F, Canon, Tokyo, Japan) [Miyazaki et al., 2018]. The sections were scanned at 4,800 pixels per inch and saved in BMP and JPG formats.

The laryngeal cartilages, tracheobronchial cartilages, and airways were segmented into serial digital sections. 3D images were computationally reconstructed, and their morphology was analyzed using Amira v.5.5.0 (Visage Imaging GmbH, Berlin, Germany).

Histological Observation

The phase of cartilage differentiation was defined according to Bucher and Reid [1961] with some modifications (Fig. 1).

Phase 1 (mesenchymal cell aggregation) consists of aggregated mesenchymal cells with a spindle form. No distinct borders are observed.

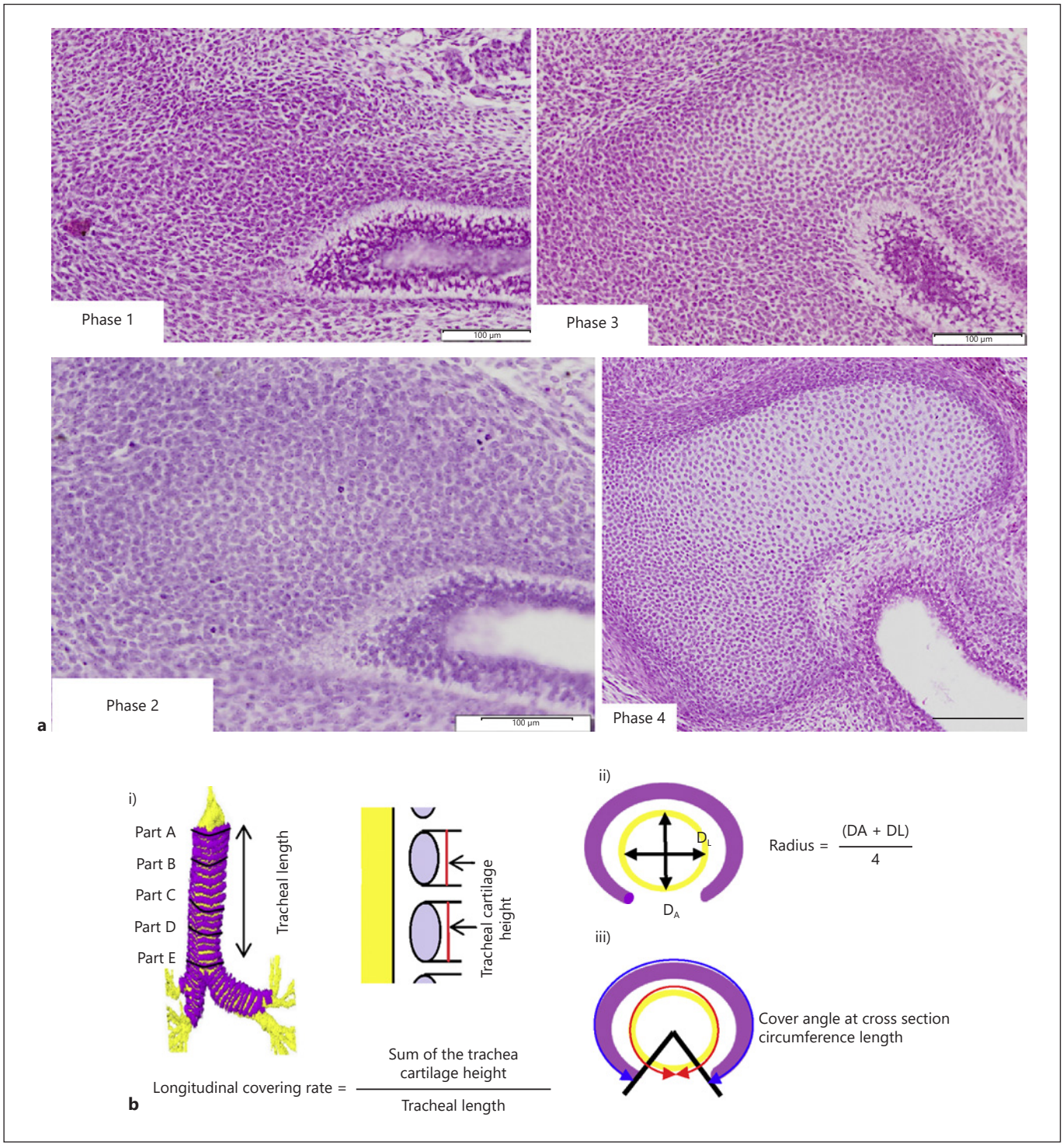

Fig. 1. Histological findings and morphometry of the tracheal cartilages. **a** Histological differentiation of the cartilage defined by 4 successive phases. Representative histology of the cricoid cartilage at CS18 (ID.1973) for phase 1, CS19 (ID.923) for phase 2, CS20 (ID.10344) for phase 3, and CS22 (ID.3147) for phase 4. Scale bars in all images represent 100 µm. **b** Illustration indicating the length and angle measurements of the trachea. i) Five transverse planes at even intervals (parts A–E) were used to measure the radius. All tracheal cartilage heights were summed and divided by the tracheal length, which was defined as the longitudinal covering rate. ii) The radius is defined as (DA + DL)/4, where DL is the lateral diameter and DA is the anteroposterior diameter. iii) Covering angle (black double line), circumference length of the trachea (red arrow), and cartilage (blue arrow).

Phase 2 (pre-cartilage_1) consists of concentrations of large cells (chondroblasts) with round, dark nuclei and palely eosinophilic cytoplasm. The borders become distinct. No cartilage matrix is detected.

Phase 3 (pre-cartilage_2): The chondroblasts become bigger, and the nuclei appear more widely separated from each other. Cartilage matrix between individual cells is detected.

Phase 4 (cartilage): A cartilage matrix gradually appears between the cells, palely stained reddish gray with HE. Groups of cells (2–4) may remain as a single unit.

Morphometry

The height of the hyoid bone, thyroid lamina, and cricoid lamina/horn were measured on the mid-sagittal plane. The circumference and covering angle of the hyoid bone, thyroid cartilage, and cricoid cartilage were measured on the horizontal plane. For thyroid cartilage, the distance between the tip of the superior horn and that of the inferior horn was measured.

Tracheal length was measured between the proximal and distal tracheal ends, which included the cartilage. The height of each tracheal cartilage was measured in the mid-sagittal plane. The sum of the tracheal cartilage height was calculated (Fig. 1b-i). The longitudinal covering rate was defined as the sum of the tracheal cartilage length per tracheal length.

The radius (Fig. 1b-ii), covering angle at the cross-section (black double line), and circumference length (red and blue arrows in Fig. 1b-iii) were measured on 5 horizontal planes at even intervals, including the proximal and distal tracheal end. The height of the second tracheal cartilage from the cranial side was used to compare the cover angle at the cross-section and circumference length between laryngeal cartilages and tracheal cartilages.

Results

Laryngeal Cartilages

Hyoid Bone

Pre-cartilage of the greater horn (phase 2) appeared at both ends at CS18 and extended to the midline (Fig. 2). Two chondrification centers in the hyoid bodies were detected closely at CS19, which fused at the medial part (triangle in Fig. 2). The hyoid body and the pre-cartilage from the greater horn were close to each other, although the borders were distinct. The cartilage matrix became conspicuous between pre-cartilage cells (phase 3) at the median part of the hyoid body at CS19, which was the earliest in all other laryngeal and tracheobronchial cartilages. The cartilage matrix was observed over almost the whole area of the hyoid bone (phase 3–4) at CS20.

Both ends of the hyoid bone (greater horn) were close to the superior thyroid cartilage during the observation period. All CS20–21 individuals had a slightly curved linear morphology. The hyoid body increased in size. In the cross-sections, the greater horn was circular, while the body was elliptical. The size of the body increased further at CS22. The border between the greater horn of the hyoid bone and the superior horn of the thyroid cartilage became clear. The lesser horn was hard to recognize as a cartilaginous form in any specimen. No ossification was observed in the hyoid bone during the observation period.

Thyroid Cartilage

Pre-cartilage (phase 2) appeared at the superior horn of the thyroid cartilage at CS18, which expanded toward the median part, forming the lateral lamina at CS19 and the following stages. In CS20, phase 3 cartilage spread from the central part of the lamina at CS20, which spread to almost all areas except the area adjacent to the greater horn of the hyoid at CS21. In CS22, the lateral lamina further extended ventrally, showing a morphology similar to that of adults. Phase 4 cartilages were formed from the central parts of the lateral laminae and expanded to both ends. In CS23, the lateral laminae were not yet fused, but phase 4 cartilage was formed in almost all areas except the fusion boundary and the superior horn, which is close to the greater horn of the hyoid bone. The laminae fused at the median part in early fetal specimens with a CRL of 39 mm and higher.

Cricoid Cartilage

Mesenchymal cells of the cricoid cartilage appeared above the upper trachea (phase 1); these boundaries were unclear at CS18 and CS19. Pre-cartilage was first visible at CS20 as U-shaped phase 3 cartilage around the cricoid arch and surrounding the subglottic cavity, which expanded to the dorsal part. The cricoid lamina elongated downward, which fused on the dorsal side at CS22. In specimens after CS22, the dorsal cricoid lamina increased in height, which was morphologically similar to that of adults. The cartilaginous phase was phase 3 at the posterior midline region at CS22, which became phase 4 in almost all regions at CS23.

Morphometry

The heights of the lamina and horn of the thyroid cartilage increased linearly during the embryonic period, and the rate of increase became gentle during the early fetal period (Fig. 3a). The height of the cricoid arch increased almost linearly during the embryonic and early fetal periods. The height of the lamina increased rapidly after fusion at CS22 (Fig. 3b).

The height of the hyoid bone, lamina of the thyroid cartilage, and arch of the cricoid cartilage and tracheal cartilage at the anterior part of the mid-sagittal section

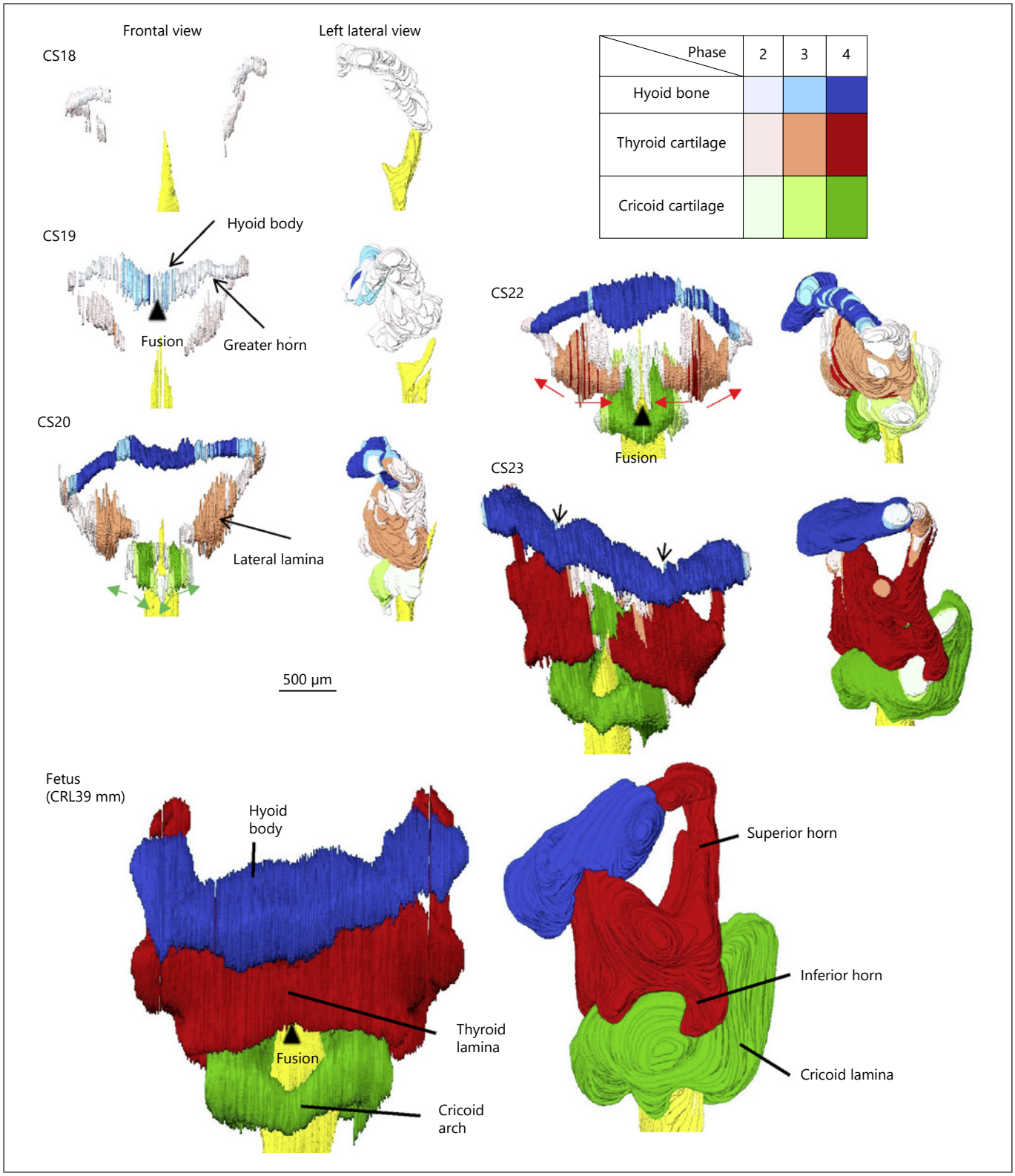

Fig. 2. 3D reconstruction of laryngeal cartilages during embryonic and fetal development. Phases of cartilage formation were surface-mapped by the colors indicated in the panel. Triangles indicate the fusion of cartilage. Arrows indicate the direction in which the cartilage differentiation proceeds.

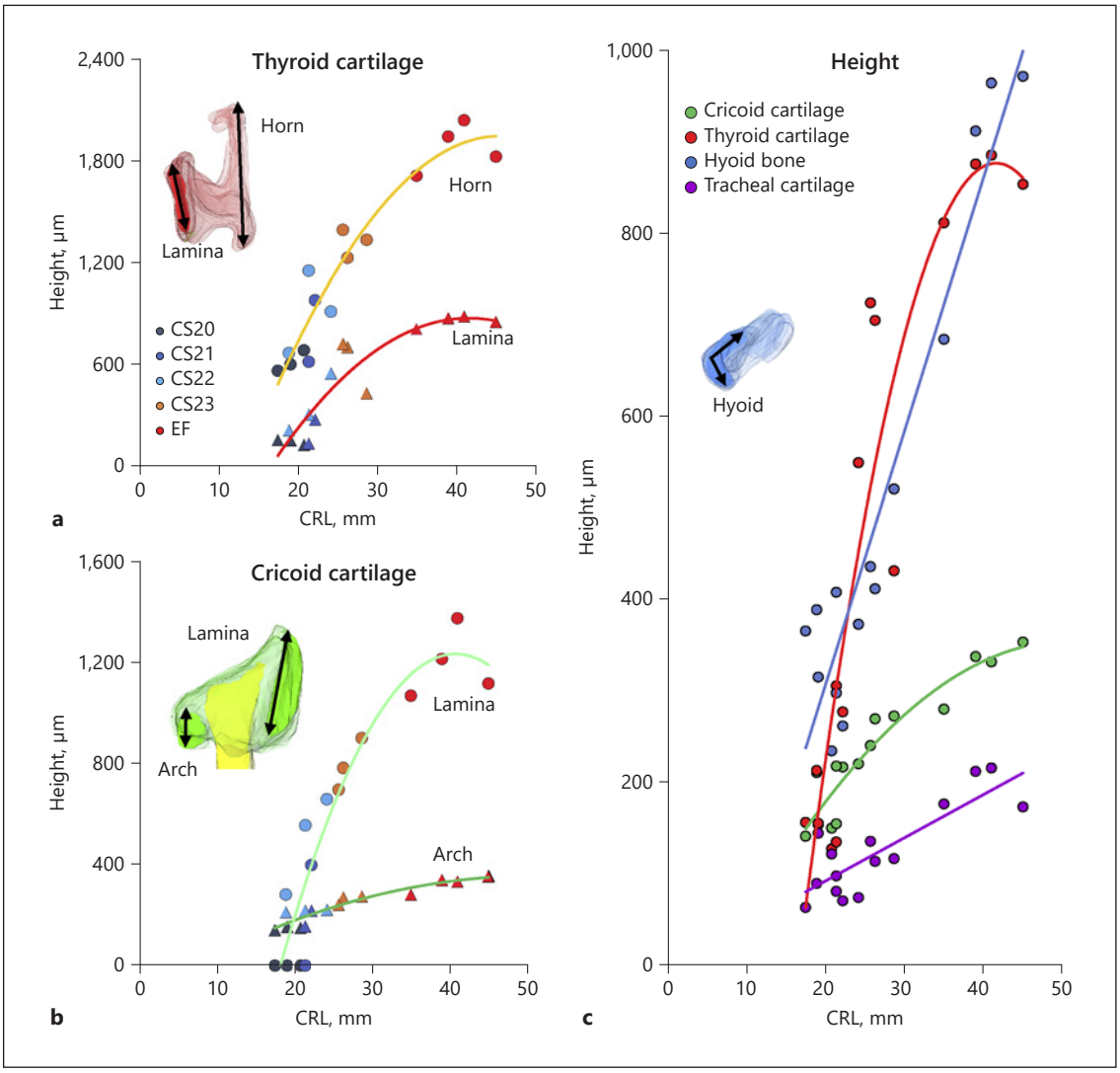

Fig. 3. Height of laryngeal cartilages. **a** Height of the lamina and horn of thyroid cartilage. **b** Height of the arch and lamina of cricoid cartilage. **c** Height of the hyoid bone (blue), lamina of thyroid cartilage (red), and arch of cricoid cartilage (green) and tracheal cartilages (purple) at the anterior part in the mid-sagittal section. The second tracheal cartilage is indicated for comparison.

were compared (Fig. 3c). The height of the thyroid cartilage and hyoid bone increased at a rapid rate, while that of the cricoid cartilage and tracheal cartilage increased slowly.

The circumference length of the laryngeal cartilages increased almost linearly during the observation period (Fig. 4a). These values and rates of increase were much higher than those of the trachea and tracheal cartilage. The rate of increase in the cricoid cartilage was comparable to that of the hyoid bone, which was higher than that of the thyroid cartilage.

The timing at which the cover rate increased at the cricoid cartilage was earlier than that at the thyroid cartilage. The thyroid cartilage covered the airway at an angle of 150–185° in the specimens with CS20–21 and increased at CS22, reaching approximately 210–250° after CS23 (Fig. 4b). The cricoid cartilage covered the subglottic cavity at an angle of approximately 180° in 2 of 3 CS20 specimens and 245° in 1 of 3 CS20 specimens and 1 of 2 CS21 specimens (Fig. 4c). The cricoid cartilage covered the entire subglottic space (i.e., 360°) in the remaining specimen at CS21 and later stage specimens.

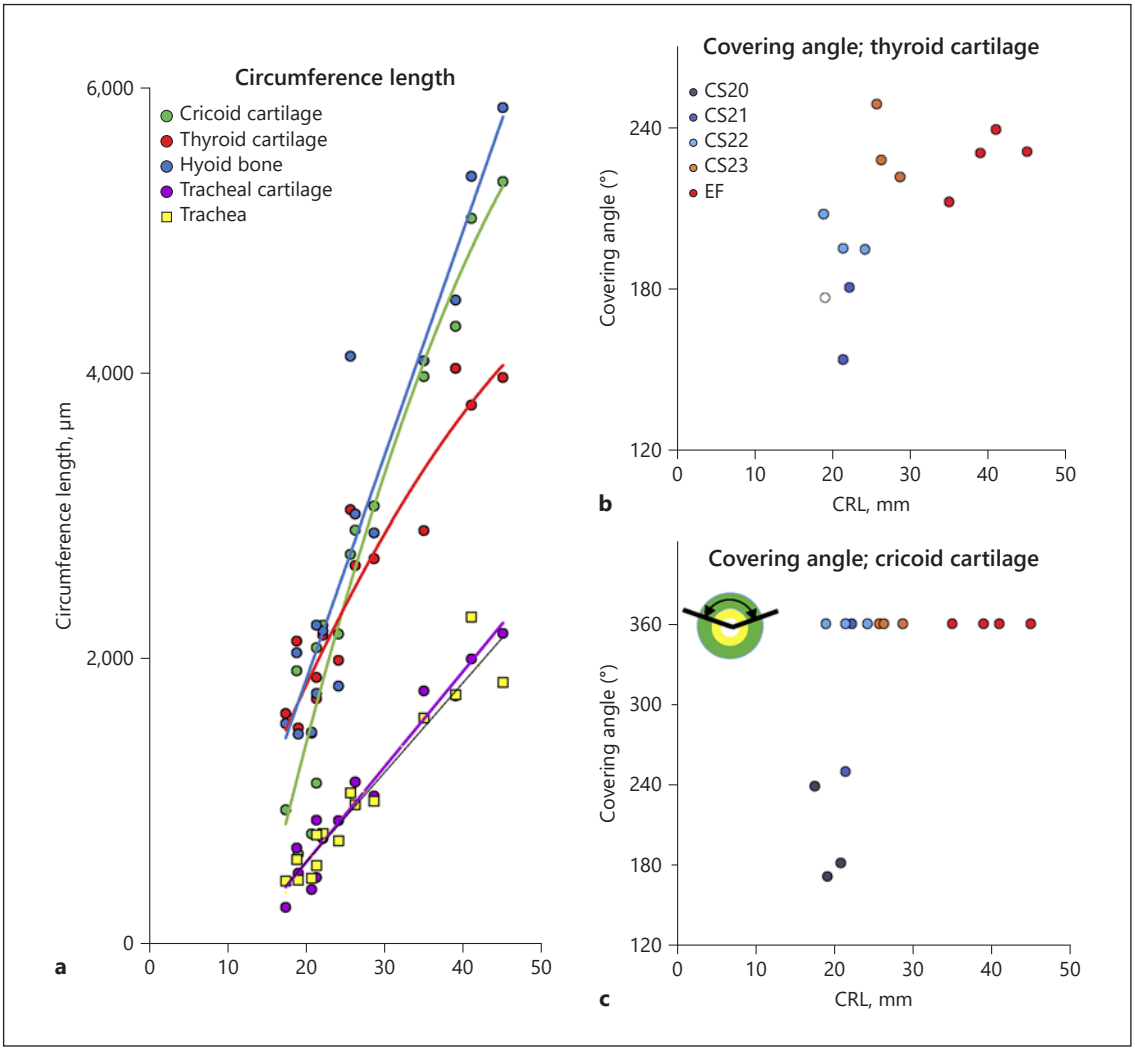

Fig. 4. Morphometry using the cross-section of the laryngeal cartilages. **a** Circumference length of thyroid cartilage (red), cricoid cartilage (green), and the hyoid bone (blue). The trachea (yellow) and trachea cartilage (purple) are indicated for comparison. **b** Covering angle of thyroid cartilage. **c** Covering angle of cricoid cartilage. An illustration showing the radius and covering angle of the cartilages is provided in Fig. 1b-ii, 1b-iii.

Tracheobronchial Cartilages

Histology of Cartilage Differentiation at Phase 1 and Phase 2

At CS18, mesenchymal cells aggregated around the trachea and bronchi. At CS19, chondroblasts appeared to surround the trachea and bronchi, but the boundary with the surrounding tissue was still unclear (phase 1) at CS19. At CS20, tracheal cartilages began to form a node structure, and boundaries with surrounding tissue became recognizable (phase 2) (Fig. 5). In the mid-sagittal section, the cranial part of the tracheal cartilages were at phase 2, while the remaining were at phase 1 in 1 specimen at CS20 (CS20_1, CRL 17.5 mm) (Fig. 5a). All tracheal cartilages were observed as a similarly histological differentiation (at phase 2) for the remaining 2 specimens at CS20 (Fig. 5b, CS20_2, CRL 19.1 mm). The first tracheal cartilage was larger than the remaining cartilages.

Tracheal Cartilages

In 1 of the 3 specimens at CS20 (CRL 17.5 mm), tracheal cartilages remained in phase 1 at the median part of the trachea (Fig. 6a, CS20_1), whereas almost all trachea cartilages were in phase 2, and the cartilage matrix was detected only to a limited extent in the remaining 2 specimens (phase

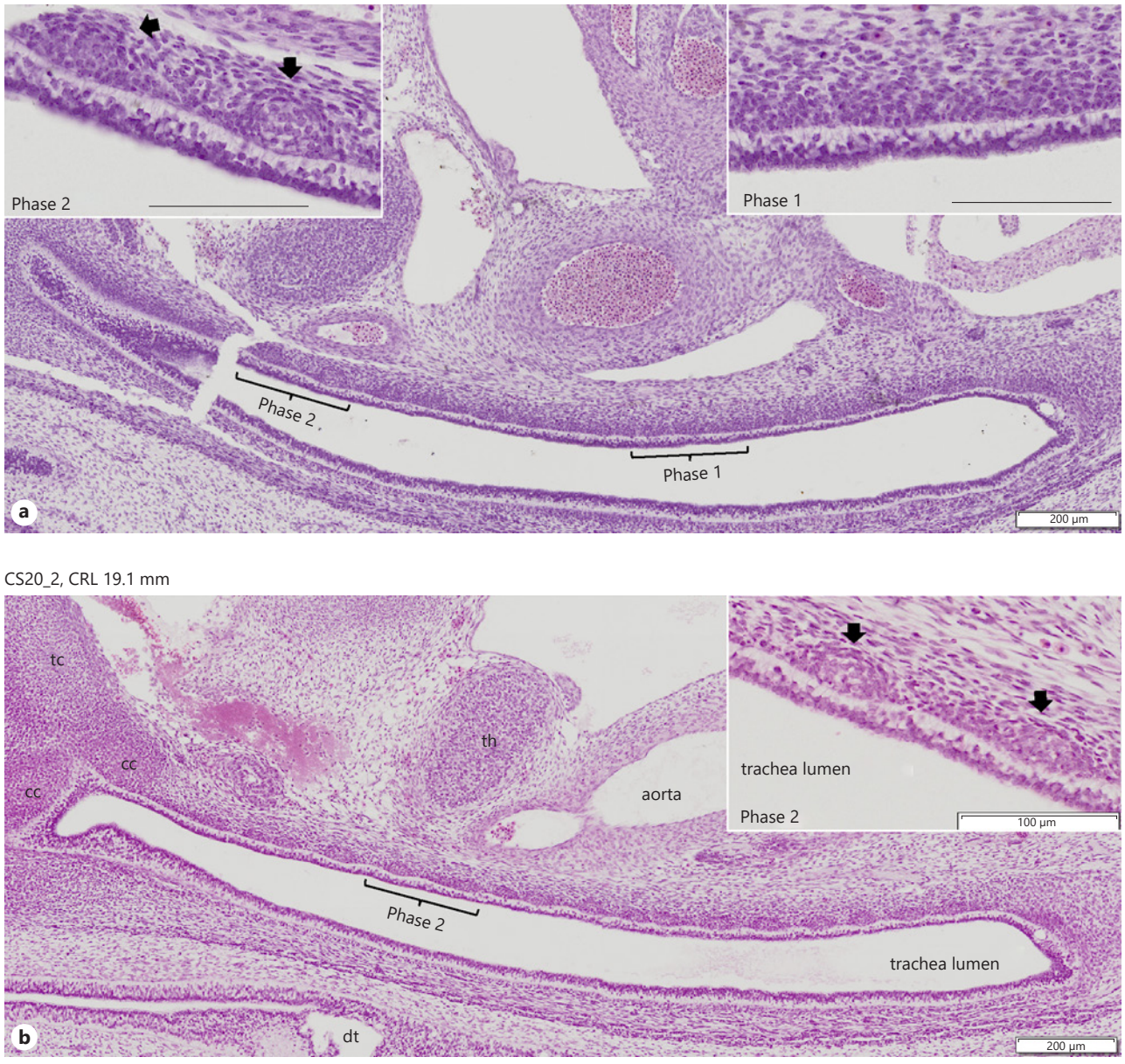

Fig. 5. Mid-sagittal tissue sections of tracheobronchial cartilages. **a** The mid-sagittal tissue section showing tracheobronchial cartilages at phase 1 and phase 2 (CS20_1, CRL 17.5 mm). In phase 1, mesenchymal cells line up beneath the tracheal epithelium, while boundaries with surrounding tissue are unclear. In phase 2, cartilage cells line up, and boundaries with the surrounding tissue become evident. Note that the several tracheal cartilages at the cranial side occurred at phase 2 while the remaining were at phase 1. **b** The mid-sagittal tissue section trachea showing tracheobronchial cartilages at phase 2 (CS20_2, CRL 19.1 mm). All 18 tracheal cartilages were similarly observed at phase 2, indicating that no difference of the histological differentiation was noted. The first tracheal cartilage is larger than the remaining cartilages. cc, cricoid cartilage; dt, digestive tract; tc, thyroid cartilage; th, thymoma.

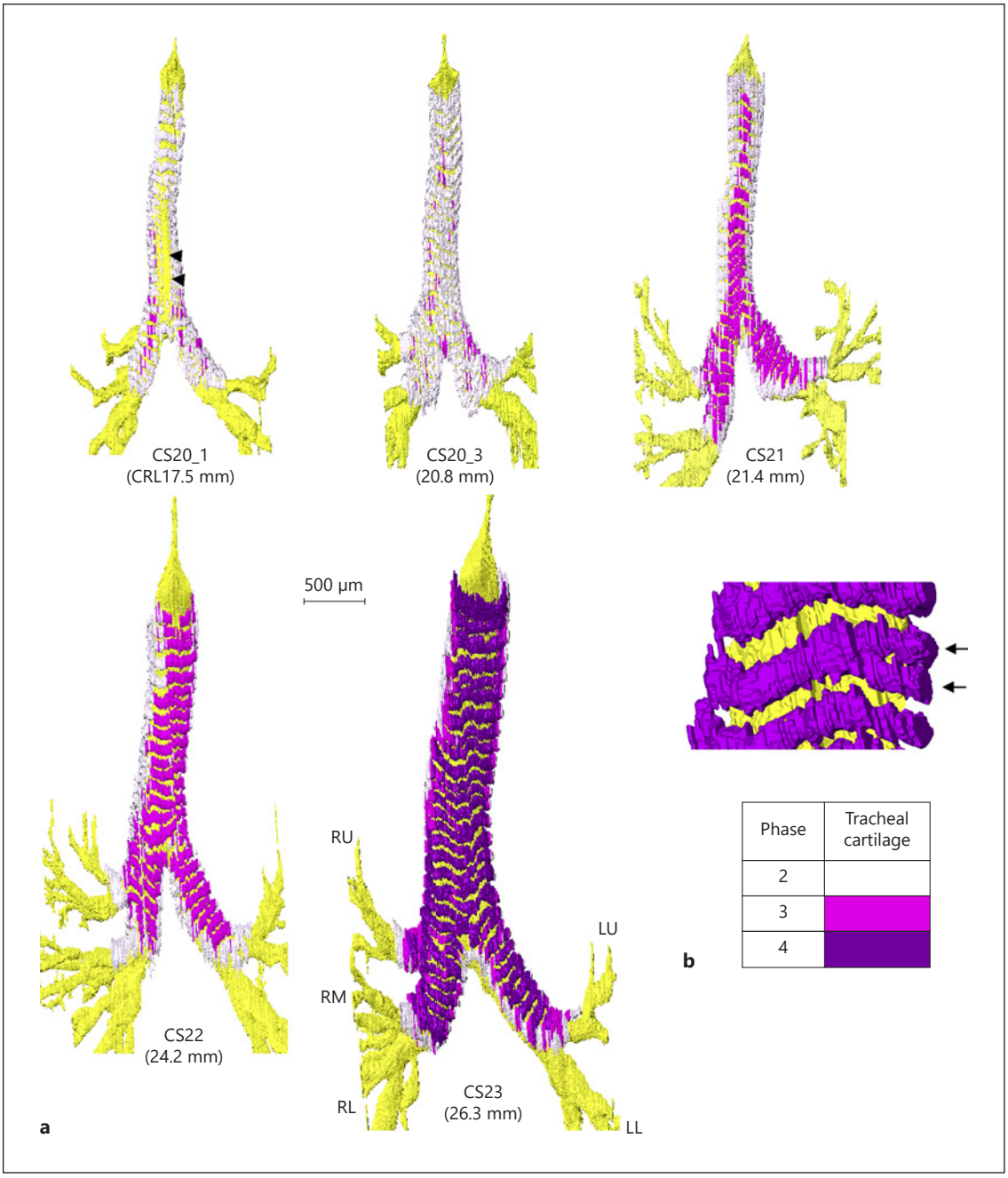

Fig. 6. Tracheobronchial cartilage formation during embryonic development. **a** 3D reconstruction of tracheobronchial cartilages (ventral view). Differentiation phases 2–4 of cartilage formation were surface-mapped by the colors indicated in the panel. LU, left upper lobe; LL, left lower lobe; RU, right upper lobe; RM, right middle lobe; RL, right lower lobe. Note that the midline portion of the tracheal cartilage did not reach phase 2 differentiation in 1 specimen at CS20_1 (CRL 17.4 mm) (arrowheads). **b** Branched tracheobronchial cartilage (arrows).

2) (Fig. 6a, CS20_3). In specimens at CS20 and later, the boundary between the cartilage and surrounding tissues was clarified. Phase 3 cartilages appeared at the median part at CS21 in all tracheal cartilages. All areas of tracheal cartilages, except for the border, became phase 3 at CS22 and phase 4 at CS23 (Fig. 6). Tracheal cartilages lined up in an orderly manner, parallel with occasional branching and fusion to the neighboring cartilage (Fig. 6b).

Table 1. Morphometry of the tracheal cartilage

	CS	ID	CRL, mm	Trachea					Main bronchi	
				Number of cartilage		Sum of tracheal cartilage height, μm	Tracheal length, μm	Longitudinal covering ratio	Number of cartilage	
				total	branched				right	left
Embryo	20	15818	17.5	19	1	788	1,521	0.52	nd	nd
		10344	19.1	18	0	1,514	1,904	0.8	nd	nd
		567	20.8	21	4	1,812	2,167	0.84	nd	nd
	21	2021	21.4	21	0	1,810	2,203	0.82	nd	nd
		7316	22.2	21	3	1,978	2,622	0.75	nd	nd
	22	10642	18.9	23	5	1,482	2,028	0.73	7	8
		6225	21.4	19	4	1,583	2,135	0.74	7	10
		3147	24.2	16	3	1,563	2,058	0.76	7	9
	23	9026	25.7	21	7	2,434	2,885	0.84	7	9
		4381	26.3	20	8	2,377	3,251	0.73	7	8
		12481	28.7	18	3	2,243	3,112	0.72	7	10
Fetus	10424	35	18	3	2,880	3,467	0.83	7	11	
	10426	39	20	2	3,806	4,490	0.85	7	9	
	10429	41	19	1	3,789	4,601	0.82	8	10	
	10430	45	19	3	3,060	3,636	0.84	9	11	

CS, Carnegie stage; CRL, crown-ramp length; LCR, longitudinal covering ratio = sum of tracheal cartilage height/tracheal length.

Morphometry

The total tracheal length increased linearly with growth. The number of tracheal cartilages was almost constant, ranging between 16 and 23 (Table 1). Both total tracheal length and the sum of each tracheal cartilage height increased linearly with growth (Fig. 7a). The longitudinal covering rate (sum of each tracheal cartilage height per total tracheal length) was also almost constant, ranging from 0.74 to 0.84 during the observation period, except for 1 small specimen at CS18. Branched cartilage was occasionally observed, ranging from 0 to 8 per specimen, which was not related to the stage of growth.

The radius of the tracheal lumen increased linearly during the observation period (Fig. 7b). The radius of the lower part (Part E) was higher than that of the mean of the remaining 4 parts (Part A–D).

The circumference of the tracheal cartilages increased linearly with growth (Fig. 7c). This value was almost comparable to that of the trachea. The tracheal cartilages covered approximately 185–230° at all specimens at CS20 and CS21 and 1 of 2 specimens at CS22, while they covered approximately 220–270° at the remaining specimen at CS22 and specimens of CS23 and early fetal period (Fig. 7d).

Bronchial Cartilages

The left and right main bronchi and the left and right upper lobe bronchi were recognizable in the specimen at CS20 and later stage specimens. The parallel lineup of the cartilage was disturbed at the carina and proximal part of the right upper lobe. Complex branching and fusion to the neighboring cartilages were observed in this region (asterisks in Fig. 8). The branching and fusion patterns varied for each specimen. The parallel lineup was mostly held at the left main bronchus, and the number of cartilages in the left main bronchus was larger than that in the right main bronchus (Table 1). The cartilage covered the cranial side of the left main bronchus and uncovered the caudal side (arrows in Fig. 8).

No U-shaped cartilage tissues were found around the middle or lower lobe bronchi or the tertiary bronchus, although irregular cartilages were occasionally formed at the end of the main bronchi and upper lobes in the specimen at CS23 and specimens of early fetal period (arrowheads in Fig. 8).

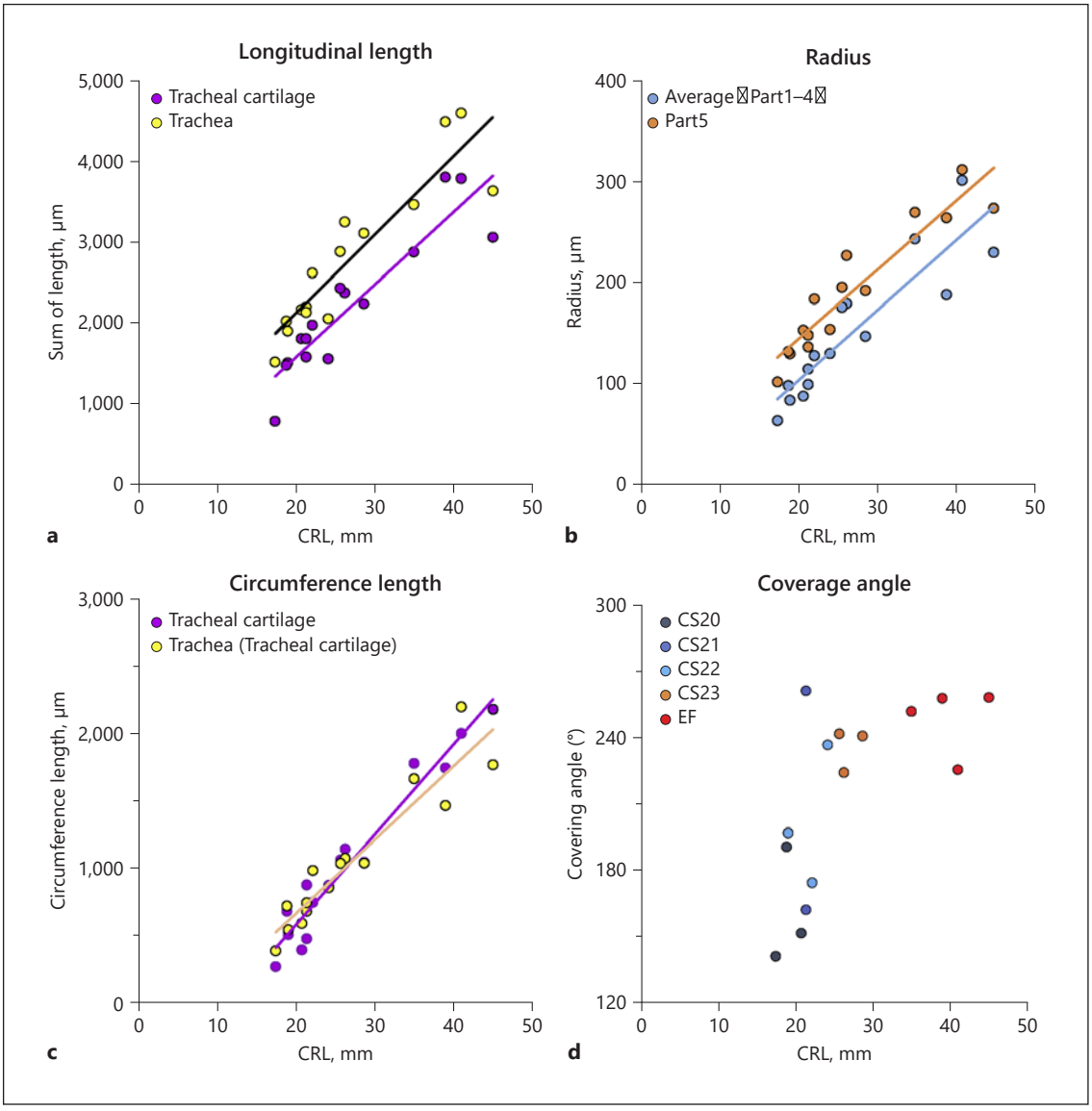

Fig. 7 Morphometry of trachea cartilages and trachea during the embryonic and early fetal period. **a** Tracheal length and sum of tracheal cartilage heights according to growth. **b** Radius of the trachea according to growth. The average radius of 5 tracheal transverse sections at even intervals was calculated for each specimen. **c** The circumference length of tracheal cartilages and trachea. **d** The covering angle of tracheal cartilages. An illustration showing the morphometry of the trachea and tracheal cartilages is provided in Figure 1b.

Discussion and Conclusion

Laryngeal Cartilages

Morphogenesis of the laryngeal region, including the first appearance of laryngeal cartilages, was described more than a century ago [Bardeen, 1910; Lisser, 1911]. Morphogenesis has been reexamined [Zaw-Tun and Burdi, 1985; Rodríguez-Vázquez et al., 2011; de Bakker et al., 2018], but the timing and morphogenesis of each laryngeal cartilage remain discrepant.

Objective and easy estimation of bone formation is possible using X-ray images, even in large areas. Thus, the timing of appearance of each ossification center and bone formation have been well described, which may be applied to the estimation of fetal and child growth [Mall, 1906; Noback and Robertson, 1951]. However, the detection of

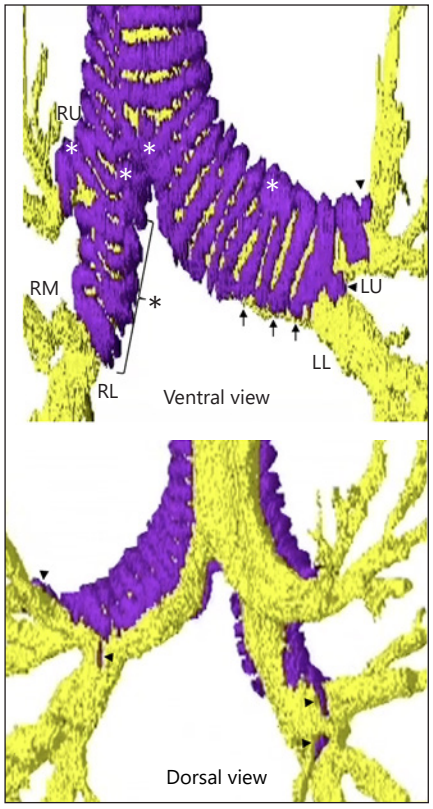

Fig. 8. Cartilage formation at the carina and main bronchi. 3D reconstruction of the specimen in the early fetal period (ID.10424, CRL 35 mm). Branching and fusion to neighboring cartilages is shown by asterisks. Cartilage uncovering the caudal side in the left main bronchi is depicted by arrows and irregular cartilages by arrow heads. LU, left upper lobe; LL, left lower lobe; RU, right upper lobe; RM, right middle lobe; RL, right lower lobe. No cartilage tissue was found around the middle or lower lobe bronchi or the tertiary bronchi.

cartilage development and differentiation depends on histological and anatomical analyses. The timing of the appearance of cartilage centers in human embryos was reported in a limited study using whole-body staining (Wijhe's method) [Noback and Boving, 1962; Tanaka, 1976], in which large individual differences were noted. Most of the cartilages were related to bone formation and little information on laryngeal and tracheobronchial cartilages formation was described. Information on cartilage formation using histological sections has been confined to a small area of the body. Recently, de Bakker et al. [2018] segmented the hyoid-larynx complex, including the first and second pharyngeal arch cartilages. The simplified development of the hyoid-larynx complex from only the second and third pharyngeal arch cartilage, in combination with a single hyoid body anlage, was described in their study. The criteria defining the timing when cartilage formation was initiated and segmented for 3D reconstruction was still unknown in their study. In our study, the degree of histological differentiation was confirmed for each histological section, and that information was mapped on the 3D reconstruction, which contributed to the comprehensible timeline of the formation of laryngeal cartilages, hyoid bone, and tracheobronchial cartilages.

The hyoid greater horns were recognizable at CS18 as a rod-like form of cartilage (phase 2). The cartilage matrix became conspicuous between pre-cartilage cells (phase 3) at the median part of the hyoid body at CS19, which was the earliest in all other laryngeal and tracheobronchial cartilages. Most of the laryngeal cartilages were phase 3 in differentiation at CS22 and phase 4 at CS23. The first differentiation center (phase 2) was not on the median plane, instead there were 2 at the lateral sides in the hyoid bone, thyroid, and cricoid cartilage. According to the respective timeline, the differentiation sites propagated fusing on the median plane. Fusion in the mid-sagittal region was observed at CS19 in the hyoid bone, at CS20 in the cricoid cartilage, and in the specimen with a CRL of 39 mm in the thyroid cartilage.

From a comparative anatomical standpoint, structures composed of the maxilla, mandible, and pharyngeal and laryngeal regions were of brachial arch origin. As for the cartilage, the first cartilage (Meckel cartilage) [Bardeen, 1910; Orliaguet et al., 1994; Rodríguez-Vázquez et al., 1997] and the second cartilage (Reichert's cartilage) have been well described [Bardeen, 1910; Rodríguez-Vázquezet al., 2006]. The first cartilage was related to mandible and ear ossicle formation, while the proximal part of the second cartilage was also related to the ear ossicle. Such a viewpoint may lead to an overestimation of cartilage formation and their interpretation. de Bakker et al. [2018] segmented all secondary cartilages (Reichert's cartilage) during the late embryonic period, which connects to the hyoid body. Hyoid greater horns were detected close to the hyoid body, which was interpreted as a third cartilage. Rodríguez-Vázquez et al. [2011] segmented the caudal part of the horn, which continues to the lesser horn, and hypothesized that the lesser horn should be of second cartilage origin. Our study presented no evidence that the laryngeal cartilages may be derived from the brachial arches. Apart from the argument of such origin of laryngeal cartilages, the hyoid greater horn is the only cartilage in a rod shape, detected as phase 2 and later in the present study. No secondary cartilage (Reichert's cartilage) or even small horns were segmented around the hyoid bone because they were not differentiated to phase 2 of the cartilage. The rod-shaped car-

tilages, which might correspond to the fourth and sixth cartilages, were not found around the thyroid and cricoid cartilage, which was consistent with a previous study. To determine the origin of laryngeal cartilages, other analyses using molecular biology and immunohistochemistry should be performed [Elluru et al., 2009].

Tracheobronchial Cartilages

The U-shaped cartilages with phase 2 differentiation covered the entire extrapulmonary region at CS20. All areas of tracheal cartilages, except for the border, became phase 3 at CS22 and phase 4 at CS23. The number of cartilages in the trachea and main bronchi were similar in studies using adults, i.e., the number of cartilages ranged from 16–20 in the trachea [Miller, 1966], 4–8 at the right main bronchus, and 8–13 at the left main bronchus [Vanpeperstraete, 1973]. Furthermore, the covering angle at transverse sections was 220–270°, and the longitudinal covering rate in the trachea was 0.74–0.84. The results indicate that the tracheobronchial cartilages may form simultaneously during the late embryonic period and early fetal period and that they are similar in adults in terms of number, distribution, and tracheal airway coverage.

Observations using serial histological sections and mapping of the histological differentiation on 3D reconstruction between CS20 and CS22 clearly indicated the detailed propagation of the tracheal cartilage differentiation along the left-right (horizontal) axis and along the cranial-caudal (body) axis. It was evident that cartilage differentiation may have propagated differently on phase 2 and phase 3 differentiations.

In 1 of the 3 specimens (CS20_1 in Fig. 6), tracheal cartilages remained in phase 1 at the median part of the trachea, while almost all tracheal cartilages were in phase 2. For the differentiation along the horizontal axis, the results of this specimen suggest that initial phase 2 differentiation of the tracheal cartilage may begin in the lateral sides at CS20 and then fuse very soon afterwards on the median plane. This fusion on the median plane is likely to be a similar process to the laryngeal cartilages mentioned above. Previous studies have described cartilage differentiation starting from 1 center on the median plane for the hyoid body [de Bakker et al., 2018], cricoid cartilage [Zaw-Tun and Burdi, 1985], and tracheal cartilage [Fockens et al., 2021]. This process might not be recognized as the initial cartilage centers were closed and fusion occurred very quickly. Previous studies were discrepant about the timing of the trachea cartilage formation according to body axis, namely from cranial to caudal [Harjeet et al., 2004] and centripetal [Fockens et al., 2021]. As demonstrated in the CS20_1 specimen in our study, initial phase 2 cartilage differentiation can proceed at the cranial side. Propagation of the cartilage differentiation from carina to the cranial direction was not recognized in our specimen (i.e., CS20_1), however, phase 2 differentiation was observed at the cartilage of the carina. The mid-sagittal histological section demonstrated the synchronized differentiations of all tracheal cartilage along the body axis at phase 2 differentiation (CS20_2 in Fig. 5). Our observation suggests that phase 2 differentiation may begin at the cranial side of tracheal cartilages, propagate along the body axis over a short time period, and become synchronized before phase 3 differentiation starts.

Phase 3 differentiation of tracheobronchial cartilage starts on the median section and propagates laterally at CS21 along the transverse axis. Phase 3 and phase 4 differentiation continued in a synchronized manner along the body axis.

No obvious cartilage formation was detected in the intrapulmonary region in this study, which confirms the findings from previous studies indicating that the timeline of cartilage formation might be totally different in the intrapulmonary regions. Intrapulmonary cartilage was formed in the specimen at approximately 11–12 weeks of gestation [Bucher and Reid, 1961] or approximately 12–13 weeks of gestation [Vanpeperstraete, 1973].

Laterality in cartilage number at the right and left main bronchi has been noted in previous studies. Brenek [1941] thought that the left lung grew faster than the right lung. Our recent study showed that the branching generation between the right and left sides was comparable [Fujii et al., 2020, 2021]. The right upper lobar bronchus gives rise to lateral branching from the right main bronchi around CS16. Such a timeline may affect the complex branching and fusion patterns of the cartilages of the right main bronchi. The bronchial length rates between the carina to the branching point of the right middle lobar bronchus and that to the branching point of the left upper lobar bronchus were almost constant, at 0.45 ± 0.08, during the embryonic period [Fujii et al., 2020, 2021]. Namely, the left main bronchi were slightly longer than the right upper and lower main bronchi. These differences might contribute in part to the different number of cartilages between the left and right sides.

The current study has some limitations that should be acknowledged. First, although tissue sections are easy to observe in detail, our quantitative histological analysis using formalin and paraffin-embedded materials may have been prone to errors. Error factors may have included degeneration during specimen handling, shrinkage by

fixation, and shearing by sectioning. Second, there was an additional scope for errors during our 3D reconstruction from digitized images. Digitized images were compiled manually with visual confirmation. Distortion may occur at the time of slicing and image stacking. We may have erred in standardizing the thickness of each section. Sagittal sections were selected in this study, which may reduce the error of length measurements in the cranial-caudal direction. However, the length measurements in other directions may still be affected.

3D reconstructions of laryngeal cartilages and tracheobronchial cartilages during the embryonic and early fetal periods are presented in this study. The degree of cartilage differentiation was mapped onto the reconstructed images, which demonstrates the comprehensible timeline of cartilage formation. This detailed knowledge of cartilage formation would be useful for better understanding of the normal development and pathophysiology of congenital airway anomalies.

Acknowledgement

The authors thank Ms. Chigako Uwabe at the Congenital Anomaly Research Center for technical assistance with handling the human embryos.

Statement of Ethics

The ethics committee of the Kyoto University Faculty and Graduate School of Medicine approved this study, which used human embryos and fetal specimens (R0316).

Conflict of Interest Statement

The authors have no conflicts of interest to declare.

Funding Sources

This study was supported by Grant No. 21K07772 from the Japan Society for the Promotion of Science.

Author Contributions

Y.Y.: data analysis/interpretation and drafting of the manuscript; T.K.: data analysis; S.Y.: acquisition of data; J.M.: acquisition of data; T.T.: concept/design, critical revision of the manuscript.

References

Bardeen CR. The development of the skeleton and of tile connective tissues. In: Keibel F, Mall FP, editors. Development of the Human Body: Manual of Human Embryology. Philadelphia: B. Lippincott Company; 1910. p. 292–453.

Brand-Saberi B, Wingender E, Rienhoff O, Viebahn C. Presenting human embryology in an international open access reference Centre (HERC). In: Yamada S, Takakuwa T, editors. The Human Embryo. Rijeka: Dermatol Intech; 2012. p. 21–34.

Brenek I. Über Knorpel- und Drüsenentwicklung im menschlichen Bronchialbaum. Z Mikrosk Anat Forsch. 1941;49:525–533.

Brien P, Dalcq A. Caracreres generaux des vertebres. Principes de leur morphologie et de leur evolution. Traite de Zoologie, XII. Paris: Masson; 1954. p. 3–201.

Bucher U, Reid L. Development of the intresegmental bronchial tree: The pattern of branching and development of cartilage at various stages of intra-uterine life. Thorax. 1961;16:207–18.

de Bakker BS, de Bakker HM, Soerdjbalie-Maikoe V, Dikkers FG. The development of the human hyoid-larynx complex revisited. Laryngoscope. 2018;128:1829–34.

Elluru RG, Thompson F, Reece A. Fibroblast growth factor 18 gives growth and directional cues to airway cartilage. Laryngoscope. 2009;119:1153–65.

Fockens MM, de Bakker BS, Oostra RJ, Dikkers FG. Development pattern of tracheal cartilage in human embryos. Clin Anat. 2021;34(5):668–72.

Fujii S, Muranaka T, Matsubayashi J, Yamada S, Yoneyama A, Takakuwa T. The bronchial tree of the human embryo: An analysis of variations in the bronchial segments. J Anat. 2020;237:311–22.

Fujii S, Muranaka T, Matsubayashi J, Yamada S, Yoneyama A, Takakuwa T. Bronchial tree of the human embryo: Categorization of the branching mode as monopodial and dipodial. PLoS One. 2021;16(1):e0245558.

Harjeet A, Sahni D, Jit I. Development of the human trachea. J Anat Soc India. 2004;53:1–3.

Hartnick CJ, Cotton RT. Congenital laryngeal anomalies. Laryngeal atresia, stenosis, webs, and clefts. Otolaryngol Clin North Am. 2000;33:1293–308.

Lisser H. Studies on the development of the human larynx. Am. J. Anat.. 1911;12(1):27–66.

Mall FP. On the ossification centers in human embryos less than one hundred days old. Am J Anat. 1906;5:422–58.

Miller WS. A Morphological study of the tracheal and bronchial cartilages. Contributions to Embryology Carnegie Institution. No. 38; 1966. p. 287–99.

Miyazaki R, Makishima H, Männer J, Sydow HG, Uwabe C, Takakuwa T, et al. Blechschmidt Collection: Revisiting specimens from a historical collection of serially sectioned human embryos and fetuses using modern imaging techniques. Congenit Anom (Kyoto). 2018;58:152–7.

Noback CR, Robertson GG. Sequences of appearance of ossification centers in the human skeleton during the first five prenatal months. Am J Anat. 1951;89:1–28.

Noback CR, Boving BG. Skeletal system. In: Altman PL, Dittmer DS, editors.Growth including Reproduction and Morphological Development. Part IX. Washington: Federation of American Societies for Experimental Biology; 1962. p. 293–5.

Orliaguet T, Darcha C, Déchelotte P, Vanneuville G. Meckel's cartilage in the human embryo and fetus. Anat Rec. 1994;238:491–7.

O'Rahilly R, Müller F. Developmental stages in human embryos: Including a revision of Streeter's Horizons and a survey of the Carnegie Collection. Washington, DC: Carnegie Institution of Washington; 1987

O'Rahilly R, Müller F. The primary tissues. In: O'Rahilly R, Müller F, editors. Human Embryology & Teratology. New York, NY: Wiley-Liss; 2001a. p. 135–61.

O'Rahilly R, Müller F. The respiratory system. In: O'Rahilly R, Müller F, editors. Human Embryology & Teratology. New York, NY: Wiley-Liss; 2001b. p. 285–98.

Rodríguez-Vázquez JF, Mérida-Velasco JR, Mérida-Velasco JA, Sánchez-Montesinos I, Espín-Ferra J, Jiménez-Collado J. Development of Meckel's cartilage in the symphyseal region in man. Anat Rec. 1997;249:249–54.

Rodríguez-Vázquez JF, Mérida-Velasco JR, Verdugo-López S, Sánchez-Montesinos I, Mérida-Velasco JA. Morphogenesis of the second pharyngeal arch cartilage (Reichert's cartilage) in human embryos. J Anat 2006;208:179–89.

Rodríguez-Vázquez JF, Kim JH, Verdugo-López S, Murakami G, Cho KH, Asakawa S, et al. Human fetal hyoid body origin revisited. J Anat. 2011;219:143–9.

Tanaka O. Time of the appearance of cartilage centers in human embryos with special reference to its individual difference. Okajimas Folia Anat Jpn. 1976;53:173–98.

Vanpeperstraete F. The cartilaginous skeleton of the bronchial tree. Adv Anat Embryol Cell Biol. 1973;48:1–80.

Yamaguchi Y, Yamada S. The Kyoto collection of human embryos and fetuses: History and recent advancements in modern methods. Cells Tissues Organs. 2018;205:314–9.

Zaw-Tun HA, Burdi AR. Reexamination of the origin and early development of the human larynx. Acta Anat (Basel). 1985;122:163–84.